THE JOURNAL OF BIOLOGICAL CHEMISTRY VOL. 281, NO. 7, pp. 4477–4485, February 17, 2006

Huntingtin and Mutant SOD1 Form Aggregate Structures with Distinct Molecular Properties in Human Cells*[S]

Received for publication, August 19, 2005, and in revised form, December 16, 2005 Published, JBC Papers in Press, December 21, 2005, DOI 10.1074/jbc.M509201200

Gen Matsumoto[1], **Soojin Kim**[2], **and Richard I. Morimoto**[3]

From the Department of Biochemistry, Molecular Biology and Cell Biology, Rice Institute for Biomedical Research, Northwestern University, Evanston, Illinois 60208

Expression of many proteins associated with neurodegenerative disease results in the appearance of misfolded species that readily adopt alternate folded states. *In vivo*, these appear as punctated subcellular structures typically referred to as aggregates or inclusion bodies. Whereas groupings of these distinct proteins into a common morphological class have been useful conceptually, there is some suggestion that aggregates are not homogeneous and can exhibit a range of biological properties. In this study, we use dynamic imaging analysis of living cells to compare the aggregation and growth properties of mutant huntingtin with polyglutamine expansions or mutant SOD1 (G85R/G93A) to examine the formation of aggregate structures and interactions with other cellular proteins. Using a dual conditional expression system for sequential expression of fluorescence-tagged proteins, we show that mutant huntingtin forms multiple intracellular cytoplasmic and nuclear structures composed of a dense core inaccessible to nascent polypeptides surrounded by a surface that stably sequesters certain transcription factors and interacts transiently with molecular chaperones. In contrast, mutant SOD1 (G85R/G93A) forms a distinct aggregate structure that is porous, through which nascent proteins diffuse. These results reveal that protein aggregates do not correspond to a single common class of subcellular structures, and rather that there may be a wide range of aggregate structures, perhaps each corresponding to the specific disease-associated protein with distinct consequences on the biochemical state of the cell.

Accumulation of abnormal protein deposits as aggregates or inclusion bodies is a common cytological feature of a number of disease states as represented by clinically related neurodegenerative diseases. The mutant proteins that initiate protein aggregates in many of these diseases have been identified: Aβ in Alzheimer disease, PrP in prion diseases, α-synuclein in Parkinson disease, huntingtin in Huntington disease, tau in tauopathy, and SOD1 in familial amyotrophic lateral sclerosis (1–3). Although these proteins do not share distinctive common features in their respective primary sequences, they have all been shown to adopt alternate conformational states and form misfolded protein structures that appear visually as aggregates and inclusion bodies that correlate with disease pathology. There is increasing evidence to support a "toxic gain-of-function" mechanism by which misfolded protein and aggregate structures lead to a dominant pathological phenotype (2, 4).

A molecular basis for proteotoxicity is the aberrant interactions between aggregation-prone proteins and other cellular proteins. This is in part supported by *in vivo* polyglutamine disease models in which aggregates have been shown to contain specific transcription factors, cytoskeletal, autophagy, and degradative proteins as well as molecular chaperones (5–14). The recruitment and sequestration of these cellular proteins has been proposed to lead to functional depletion as described for the transcription factors TATA-binding protein (TBP),[4] CREB-binding protein (CBP), Sp1 (specificity protein 1), and TBP-associated factor (TAFII130) (15–20). Sequestration of TBP and CBP is of particular interest, since both proteins contain 37 or 18 glutamine repeats, respectively. Toxic sequestration models have also been suggested for familial amyotrophic lateral sclerosis, Alzheimer disease, and Parkinson disease, although the basis for these heterologous molecular interactions is less well established (21–25). Elucidating the molecular events that occur during a process of recruitment, therefore, becomes essential to understand the mechanisms underlying protein aggregate pathology.

Seeding, growth, and recruitment properties of protein aggregates have been investigated extensively *in vitro* using purified recombinant proteins and has led to an understanding of intrinsic self-assembly pathways (26–29). However, to what extent are these *in vitro* observations informative of the *in vivo* events associated with the appearance and formation of aggregates in the cell? A major distinction between aggregate formation *in vitro* and *in vivo* is the presence of a plethora of other proteins within the cell of diverse conformational states and sequence composition. Consequently, the properties of aggregates will be influenced by multiple factors such as intrinsic rate of self-association, small molecule ligands, post-translational modifications, association with other cellular proteins that share related structural motifs, interactions with molecular chaperones, and association with degradation machinery (11, 15, 17, 18, 26, 28, 30–36).

We have shown previously that heat shock protein 70 (Hsp70) associates transiently with the surface of polyglutamine aggregates and suggested that the activity of this chaperone reflects the presence of nonnative substrates to which Hsp70 binds on the aggregate surface (14). Recent *in vitro* studies show that the interaction of TBP with huntingtin is, indeed, prevented by Hsp70 (16). This also suggests that protein aggregates *in vivo* may contain specific sites and surfaces to which nascent proteins become associated, whether transiently or irreversibly. Here, we show that the intracellular structures of mutant huntingtin

* This study was supported by grants from the National Institutes of Health (NIH) (NIGMS and NIA), the Huntington Disease Society of America Coalition for the Cure, the ALS Association, and the Daniel F. and Ada L. Rice Foundation (to R. I. M.). The costs of publication of this article were defrayed in part by the payment of page charges. This article must therefore be hereby marked "*advertisement*" in accordance with 18 U.S.C. Section 1734 solely to indicate this fact.

[S] The on-line version of this article (available at http://www.jbc.org) contains supplemental Figs. S1–S3.

[1] Supported by a Human Frontier Science Program Organization long term fellowship.

[2] Supported by the Mechanisms in Aging and Dementia Training Program of the NIA, NIH.

[3] To whom correspondence should be addressed: Dept. of Biochemistry, Molecular Biology and Cell Biology, Rice Institute for Biomedical Research, Northwestern University, Evanston, IL 60208. Tel.: 847-491-3340; Fax: 847-491-4461; E-mail: r-morimoto@northwestern.edu.

[4] The abbreviations used are: TBP, TATA-binding protein; CBP, CREB-binding protein; YFP, yellow fluorescent protein; CFP, cyan fluorescent protein; FRAP, fluorescent recovery after photobleaching; FLIP, fluorescence loss in photobleaching; RFI, relative fluorescence intensity; TRE, tetracycline response element; FRET, fluorescence resonance energy transfer.

aggregates consist of distinct layers with an inner dense core and a recruitment surface to which nascent proteins become associated in transfected cultured cells. Since these layers are not exchangeable with each other, mutant huntingtin proteins in the core are completely separated from cellular proteins. In contrast, mutant SOD1 (G85R/G93A) forms porous structures into which nascent proteins can diffuse and associate. These results demonstrate, for the first time, in a comparative analysis that different disease-associated proteins form distinct classes of aggregate structures and consequently associate differentially with other cellular proteins.

MATERIALS AND METHODS

Constructs—The pEYFP-N1-TBP and pEYFP-N1-HSP70 constructs were previously described (14). pEYFP-C1-CBP was generated by subcloning BamHI-digested CBP fragment from pRc/RSV-mCBP-HA-RK (37) into the BglII site of pEYFP-C1. The pTRE-YFP or pTRE-CFP vectors were generated by PCR amplification of YFP from pEYFP-N1 or CFP from pECFP-N1 (Clontech, BD Biosciences) using the forward primer 5′-TTTCAGCTGCAGGCTAGCGCTAGCAAGGGCGAGG-3′ and reverse primer 5′-TTAGCTAGCACGCGTTTACTTGTACAGCTCG-3′ and subcloning into the PvuII/MluI sites of pTRE2hyg (Clontech, BD Biosciences, CA). To construct pTRE-httQ78-YFP, pTRE-httQ78-CFP, and pTRE-httQ23-YFP, the respective BamHI/SphI-digested httQ150 or httQ23 fragments from pcDNA3-Q150 or pcDNA3-Q23 (gift from Dr. M. Macdonald (Harvard University)) were subcloned into the BamHI/PvuII sites of pTRE-YFP or pTRE-CFP vector. DNA sequence analysis revealed a deletion of the httQ150 construct from 150 CAG repeats to 78 repeats, resulting in pTRE-httQ78-YFP and pTRE-httQ78-CFP. pTRE-SOD1-wt-YFP, pTRE-SOD1-wt-CFP, pTRE-SOD1-G85R-YFP, and pTRE-SOD1-G85R-CFP were generated by PCR amplification of wild type SOD1 and G85R mutant SOD1 from plQL01 or plQL03 (gift from Dr. Q. Liu, Harvard Medical School), respectively, using the forward primer 5′-CTCCACCGCGGATCCATGGCGACGAAGGCCGTGTG-3′ and reverse primer 5′-TTTCAGCTGCAGTTGGGCGATCCCAATTACAC-3′ and inserting into BamHI/PvuII sites of pTRE-YFP or pTRE-CFP. pTRE-SOD1-G93A-YFP and pTRE-SOD1-G93A-CFP were generated by PCR-based site-directed mutagenesis using the forward primer 5′-GTGACTGCTGACAAAGATGCTGTGGCCGATGTGTCTATTG-3′ and the reverse complement primer 5′-CAATAGACACATCGGCCACAGCATCTTTGTCAGCAGTCAC-3′ to change glycine at amino acid residue 93 to alanine of pTRE-SOD1-wt-YFP or pTRE-SOD1-wt-CFP. The pLac/MCS vector was generated by introducing a multiple cloning site into the NotI site of pOPRSVCAT (Stratagene) using the synthesized oligonucleotides, 5′-GGCCGGTACCAGATCTCATATGGATATCCTCGAGACGCGTTCTAGAGC-3′ and 5′- GGCCGCTCTAGAACGCGTCTCGAGGATATCCATATGAGATCTGGTACC-3′. The pLac-httQ78-YFP, pLac-httQ78-CFP, pLac-SOD1-G85R-YFP, and pLac-SOD1-G93A-YFP were generated by insertion of BamHI/BglII-digested httQ78-YFP, httQ78-CFP, SOD1-G85R-YFP, or SOD1-G93A-YFP fragments from the respective pTRE- constructs into the BglII site of pLacO/MCS. The BamHI fragment containing the *lac* operator-2 was subsequently removed from each construct, since we observed an enhanced level of induction with this deletion. The pLac-TBP-YFP and pLac-Hsp70-YFP were generated by subcloning a BglII/NotI-digested TBP-YFP fragment from pEYFP-N1-TBP or Hsp70-YFP fragment from pEYFP-N1-Hsp70 into the BglII/NotI sites of pLac/MCS. To construct pLac-CBP-YFP, pLac-EYFP-C1 was first generated by cloning the NheI/BclI-digested YFP fragment from pEYFP-C1 (Clontech, BD Biosciences) into blunt-ended HindIII/BglII sites of pLacO/MCS. The pLac-CBP-YFP was then constructed by subcloning a BamHI-digested CBP fragment from pRc/RSV-mCBP-HA-RK into the BglII site of pLac-EYFP-C1. All constructs were verified by sequencing.

Cell Culture and Sequential Expression by the Dual Conditional Protein Expression System—HeTOFLI cells were generated by transfecting HeLa Tet-Off cells (Clontech, BD Biosciences) with the pCMV-LacI-NLS construct (Stratagene) using Lipofectamine PLUS reagent (Invitrogen) and selecting with 0.5 mg/ml hygromycin. The HeTOFLI cell line was maintained in Dulbecco's modified Eagle's medium supplemented with 10% fetal bovine serum, 100 units/ml penicillin, 0.1 mg/ml streptomycin, 0.2 mg/ml G418, and 0.5 mg/ml hygromycin at 37 °C in an atmosphere of 5% CO_2, 95% air. For co-localization studies, cells were grown in 2-well glass slide chambers (Lab-Tek). For live cell analysis, cells were grown in 35-mm glass bottom cell culture dishes (MatTek Corp.). Transient transfections were performed using Lipofectamine-PLUS reagent, as described in the protocol provided by the manufacturer. pTRE- and pLacO- constructs were co-transfected into HeTOFLI cells at ratios of 2:3. pTRE- and pEYFP- constructs were co-transfected into HeTOFLI cells at ratio of 2:1. For sequential expression, the transfected HeTOFLI cells were incubated for 24 h in the absence of doxycycline, and then the protein expression from the tetracycline response element (TRE) promoter was down-regulated by adding 1 μg/ml doxycycline, and expression from the Lac promoter was simultaneously induced by adding 30 mM isopropyl-β-D-thiogalactopyranoside. Samples were analyzed 12 h after the isopropyl-β-D-thiogalactopyranoside induction.

Visualization of YFP- and CFP-tagged Protein and Live Cell Imaging—Transfected HeTOFLI cells were fixed in 4% formaldehyde in 1× phosphate-buffered saline for 10 min, quenched in 0.1 M Tris-HCl, pH 8.0, for 5 min, washed in 1× phosphate-buffered saline at room temperature, and mounted in Vectashield anti-fading solution (Vector Laboratories, Inc.). Fixed samples were examined using a Leica TCS SP2/Leica DM-IRE2 inverted confocal microscope equipped with a × 63 oil objective lens (Leica Microsystems Inc.). For live cell imaging, cells were maintained at 37 °C for the duration of the experiment. Fluorescent recovery after photobleaching (FRAP) analysis was performed on a Zeiss LSM510 Axiovert confocal microscope (Carl Zeiss MicroImaging Inc.) as described previously with the following modifications: an area of 12.5 μm^2 was photobleached for 3 s (20 iterations) with 514-nm laser wavelength at 100% laser power, and single scan images were collected before and every 3 s after photobleaching at 5× zoom power (14). Fluorescence loss in photobleaching (FLIP) analysis was performed using a Leica TCS SP2/Leica DM-IRE2 inverted confocal microscope equipped with × 63 oil objective lens, and images were taken at 4× zoom before photobleaching and every 30 s while photobleaching an 8.4-μm^2 region continuously with 514-nm laser wavelength at 100% laser power. Average fluorescence intensity of the aggregates in FRAP and FLIP analysis was determined using Metamorph software (Universal Imaging Corp.). Relative fluorescence intensity (RFI) for FRAP and FLIP was determined using the equation, $RFI = ((Ne_t/N1_t)/(Ne_0/N1_0)) \times 100$, where Ne_t is the average intensity of an aggregate at a given time point and $N1_t$ is the average intensity of a nonphotobleached area of the aggregate at the corresponding time points as a control for general photobleaching (14, 38). Ne_0 and $N1_0$ represent the average intensity before photobleaching of the bleached or nonbleached area, respectively. RFI values are the average of at least three data points. All images were processed by Adobe Photoshop software (Adobe Systems Inc.).

Fluorescence Resonance Energy Transfer (FRET) Analysis—FRET analysis was carried out with Leica inverted microscope (DM-IRE2) with a × 63 objective. CFP (430-nm excitation/470-nm emission), YFP

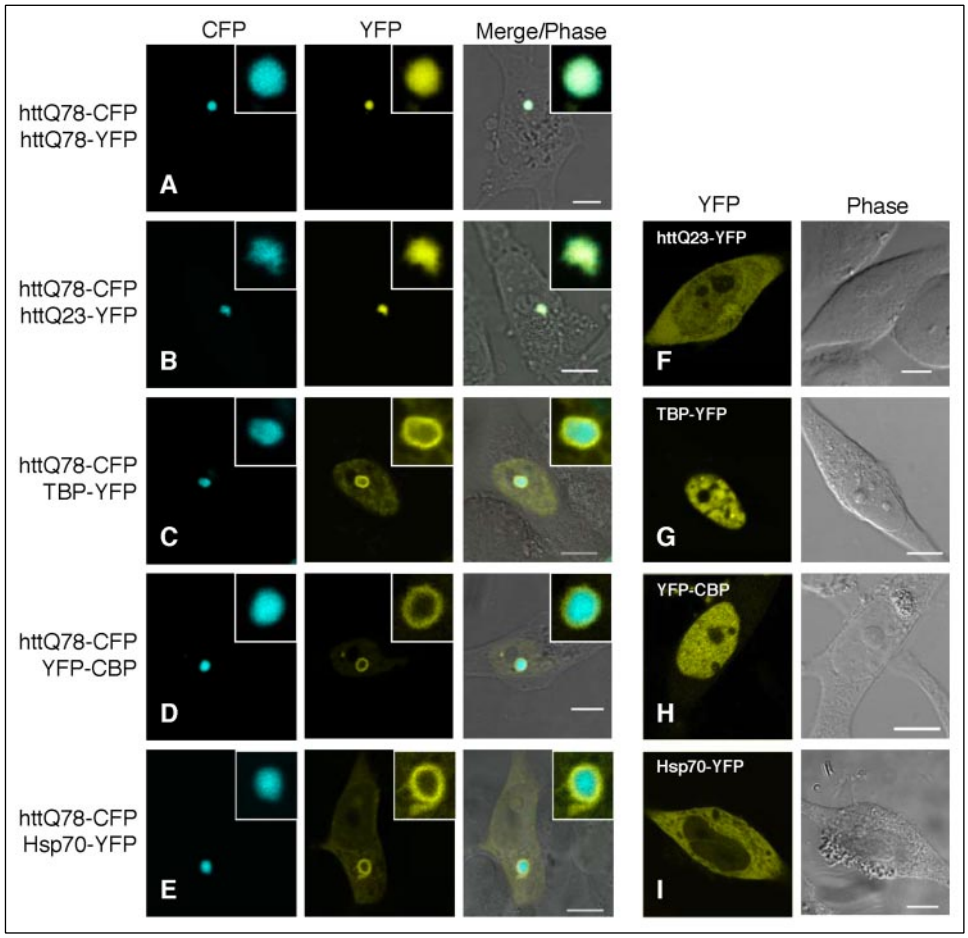

FIGURE 1. **Cellular proteins accumulate at the surface of the huntingtin aggregates.** HeTOFLI were co-transfected with constructs encoding httQ78-CFP together with httQ78-YFP (*A*), httQ23-YFP (*B*), TBP-YFP (*C*), YFP-CBP (*D*), or Hsp70-YFP (*E*). Cells with huntingtin aggregates (*CFP*) and YFP fusion proteins (*YFP*) were visualized by confocal microscopy. Co-localization was illustrated by merging CFP and YFP images and overlaying to the corresponding phase image (*Merge/Phase*). *F–I*, HeTOFLI were transfected with httQ23-YFP (*I*), TBP-YFP (*G*), YFP-CBP (*H*), or Hsp70-YFP alone (*I*). The localization of YFP-fused proteins was visualized as indicated (*YFP*, *Phase*). *Scale bar*, 10 μm.

(500-nm excitation/535-nm emission) and FRET (430-nm excitation/535-nm emission) channel images were taken with the beam splitter 86002v2 JP4 for CFP (excitation 430/25 nm and emission 470/30 nm) and YFP (excitation 500/20 nm and emission 535/30 nm) (Chroma Technology Corp.). The acquired images were then analyzed using Metamorph imaging software with the equation, $FRET^C = (FRET - 95) - 0.46(CFP - 95) - 0.016(YFP - 100) - 8$ (14, 39). The FRET ratio image was then generated by calculating the ratio between $FRET^C$ (corrected FRET) and CFP images, ranging from 0 to 3.

RESULTS

Detection of "Ring" Structures Formed by Co-expression of TBP, CBP, and Hsp70 with httQ78—To monitor the properties of huntingtin aggregates and their growth *in vivo*, we expressed the amino-terminal fragment of huntingtin shown to be associated with the appearance of aggregates and inclusions in Huntington disease (40, 41). These huntingtin constructs containing 78 glutamine repeats and tagged with either YFP or CFP (httQ78-YFP, httQ78-CFP) or 23 glutamine repeats (httQ23-YFP) were used to examine interactions with the polyglutamine aggregate-associated proteins, TBP (TBP-YFP), CBP (YFP-CBP), and Hsp70 (Hsp70-YFP). These chimera proteins are functional as previously described (14, 42–45). Co-expression of httQ78-YFP and httQ78-CFP resulted in the appearance of aggregates with both proteins uniformly distributed throughout (Fig. 1*A*), whereas HttQ23-YFP and Hsp70-YFP were diffuse in the cytosol, and TBP-YFP and YFP-CBP were localized to the nucleus (Fig. 1, *F–I*).

The subcellular distribution of httQ23-YFP, TBP-YFP, YFP-CBP, and Hsp70-YFP are all strikingly altered, however, when co-expressed with httQ78-CFP. For TBP, CBP, and Hsp70, their subcellular localization is visualized by confocal microscopy in nearly all cells (81, 100, and 94%, respectively, for TBP, CBP, and Hsp70) as a "ring" surrounding a core structure composed of the huntingtin aggregate (Fig. 1, *C–E*). Co-localization of these transcription factors is not due to the presence of YFP, since YFP alone does not associate with the huntingtin aggregate but rather is excluded from the aggregates (supplemental Fig. S1*A*). Moreover, endogenous TBP (supplemental Fig. S1*B*) and CBP (18) also co-localize with the "ring" structure of huntingtin aggregates, demonstrating that recruitment of the transcription factors is due to the intrinsic properties of these transcription factors rather than a consequence of chimeras with YFP or CFP. In contrast, httQ23-YFP co-associated with httQ78-CFP only in the core and did not form ring structures similar to the pattern of co-localization observed for httQ78 self-association (Fig. 1*B*). Taken together, these results suggest that the structure of the aggregate core is composed preferentially of huntingtin protein with polyglutamine expansions. TBP and CBP appear to be excluded from this core despite both transcription factors containing polyglutamine expansions. This suggests that the process in which cellular proteins are recruited to a polyglutamine aggregate must be influenced strongly by other properties of cellular proteins, such as the sequences adjacent to the polyglutamine expansion or other structural features.

Establishing a Dual Conditional System for the Sequential Expression of Proteins Recruited to the Surface of Huntingtin Aggregates—To test directly whether huntingtin aggregates have localized surfaces for recruitment of nascent proteins, it was necessary to establish a dual conditional protein expression system to allow for the sequential expression of CFP- or YFP-tagged proteins. The dual conditional pro-

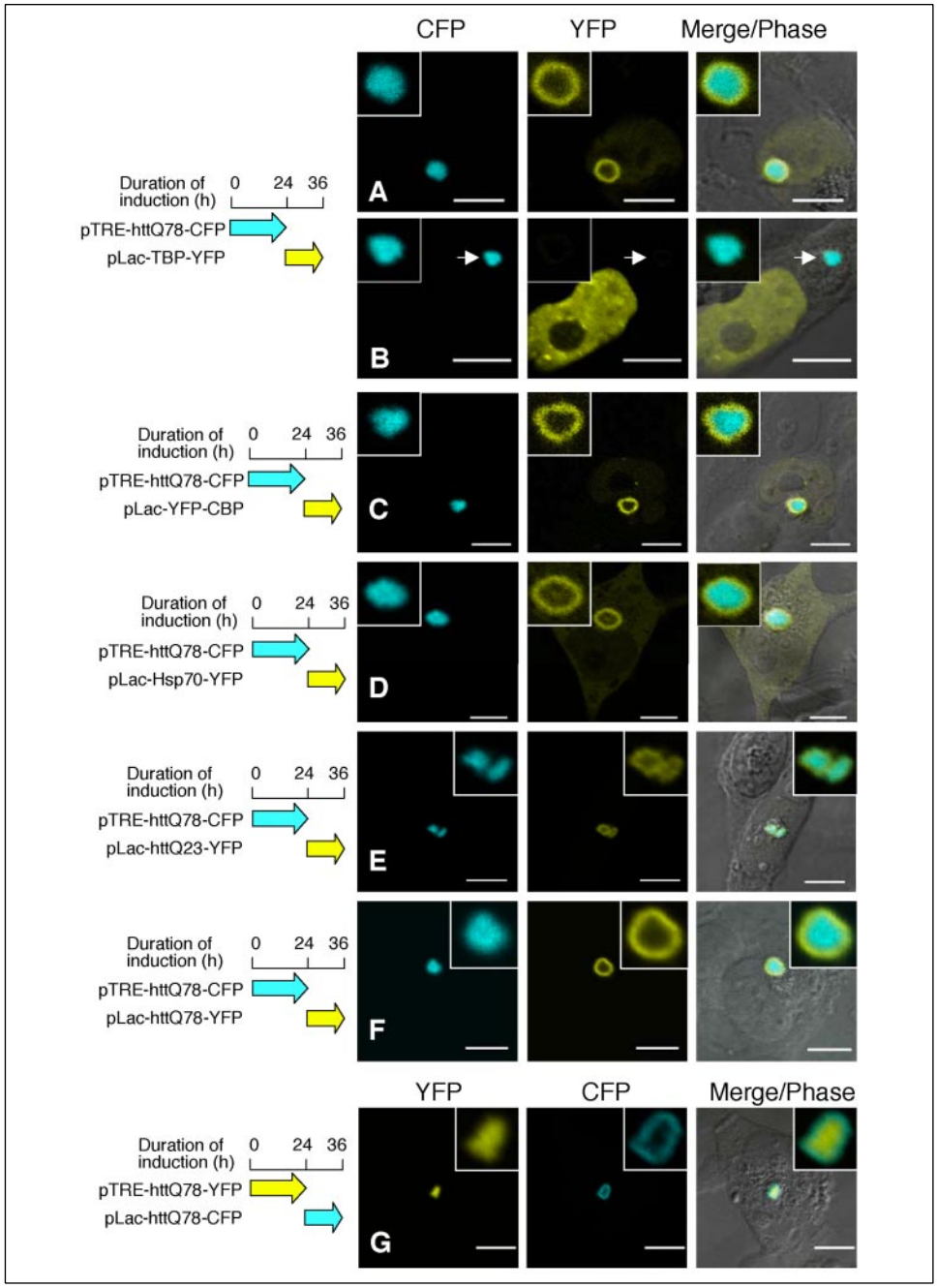

FIGURE 2. **Huntingtin aggregates contain a distinct nascent protein recruitment surface.** HeTOFLI cells were co-transfected with pTRE-httQ78-CFP together with pLac-TBP-YFP (*A* and *B*), pLac-YFP-CBP (*C*), pLac-Hsp70-YFP (*D*), pLac-httQ23-YFP (*E*), or pLac-httQ78-YFP (*F*), and sequential expression was carried out as indicated. Cells with huntingtin aggregates (*CFP*) and the YFP-fused protein (*YFP*) were visualized using a confocal microscope. The *arrows* in *B* indicate a cytoplasmic aggregate. The degree of co-localization was illustrated by merging CFP and YFP images and overlaying to the corresponding phase image (*Merge/Phase*). *G*, pTRE-httQ78-CFP and pLac-httQ78-YFP were co-transfected into HeTOFLI, and the proteins were sequentially expressed and visualized as described above. *Scale bar*, 10 μm.

tein expression system employed the Tet-off and Lac regulatory systems in which tTA and LacO-NLS stably expressing HeLa cells (HeTOFLI) was used to express two different genes under the control of the TRE or RSV-LacO (Lac) promoters (supplemental Fig. S2). With this system, we reasoned that it would then be possible to address whether proteins either co-expressed or sequentially expressed formed homogenous or heterogeneous aggregate structures. The initial expression of httQ78 would allow formation of a visual seeding structure, and the subsequent expression of an aggregate-associated protein would allow us to address the process of protein recruitment.

In vivo sequential imaging analysis was performed on cells co-transfected with pTRE-httQ78-CFP and either pLac-TBP-YFP, pLac-YFP-CBP, or pLac-Hsp70-YFP. HttQ78-CFP was expressed for 24 h, after which its expression was repressed, and the expression of TBP-YFP, YFP-CBP, or Hsp70-YFP was subsequently induced. Newly synthesized TBP-YFP and YFP-CBP were recruited efficiently to the exterior surface of nuclear aggregates and detected as YFP "ring" structures surrounding a CFP huntingtin core (Fig. 2, *A–C*). The appearance of TBP-YFP "ring" structures was less frequently detected in cytoplasmic or perinuclear aggregates than in nuclear aggregates (Fig. 2*B*), consistent with the expectation that interactions between huntingtin aggregates and transcription factors is a more frequent event in the nuclear compartment. In contrast, Hsp70-YFP was detected on the surface of both nuclear and cytoplasmic aggregates (Fig. 2*D*). These results demonstrate that the "ring" structures observed in cells expressing poly(Q)-containing proteins are, indeed, due to recruitment of cellular proteins to the exterior surface of the aggregate and moreover that the huntingtin aggregate continues to recruit other cellular protein even when expression of huntingtin is repressed.

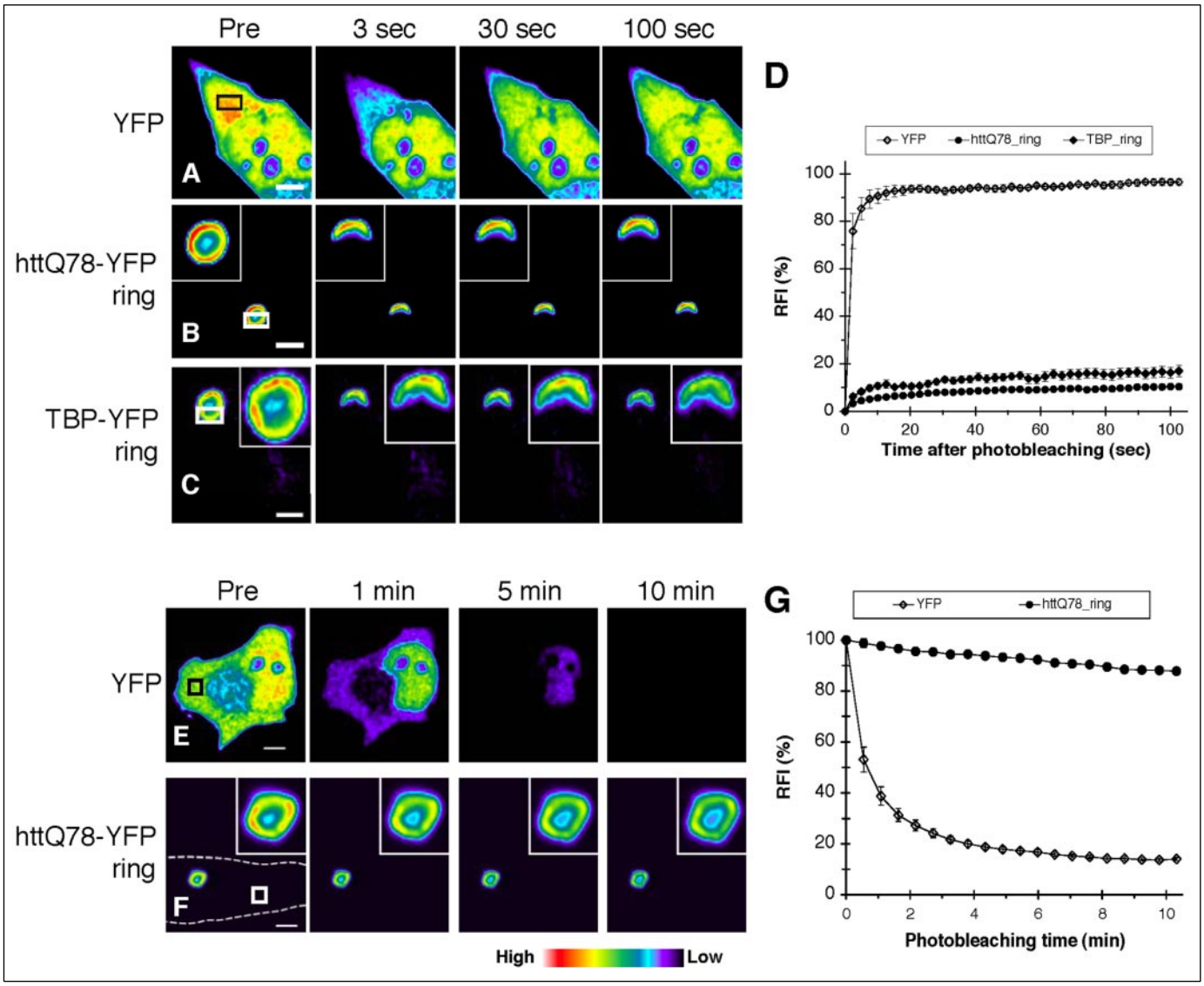

FIGURE 3. **FRAP and FLIP analysis of the recruitment surface of mutant huntingtin.** HeTOFLI cells were transfected with pTRE-YFP alone (*A* and *E*) or co-transfected with pTRE-httQ78-CFP and pLac-httQ78-YFP (*B* and *F*) or pTRE-httQ78-CFP and pLac-TBP-YFP (*C*). Sequential expression was carried out in cells transfected with pTRE-httQ78-CFP and pLac-httQ78-YFP (*B* and *F*) or pTRE-httQ78-CFP and pLac-TBP-YFP constructs (*C*) as described previously. *A–D*, for FRAP analysis, YFP-fused proteins in the *boxed area* were subjected to FRAP analysis. Single scan images were taken before (*Pre*) and at the indicated time after photobleaching. *D*, quantitative FRAP analysis is shown in the *graph*. RFI in the *boxed area* was determined for each time point (3 s) and is represented as the average of at least three cells. *E–G*, for FLIP analysis, images were taken before (*Pre*) and at the indicated time points during continuous photobleaching of the *boxed area*. RFI of the aggregates was determined for each time point (30 s) and represented as the average of at least five cells. *Error bars*, S.E. *Arrows*, mutant SOD1 aggregate. *Scale bar*, 5 μm.

To address whether the recruitment surface to which heterologous proteins associates also corresponds to sites of interaction with nascent huntingtin, we performed sequential expression studies in which httQ23-YFP or htt78-YFP was subsequently expressed after httQ78-CFP seeds were preformed. In contrast to the homogenous distribution of huntingtin in aggregates during co-expression, we observed that the sequential expression of huntingtin leads to formation of "ring" structures in 50% of the aggregates (Fig. 2, *E* and *F*). These "ring" structures were observed in both the cytoplasm and nucleus; moreover, fluorescent rings were observed regardless of the order of expression of the YFP or CFP-tagged httQ78 proteins (Fig. 2*F*). These results show that preformed huntingtin aggregates have an exterior surface that can associate with nascent mutant or wild type huntingtin and other heterologous polyglutamine containing proteins. Furthermore, the appearance of huntingtin-containing "ring" structures suggests that the huntingtin protein in the core structure does not exchange freely with proteins at the surface.

Polyglutamine-containing Transcription Factors Are Associated Irreversibly at the Surface of Huntingtin Aggregates—Our observations reveal that huntingtin aggregates contain specific sites on the exterior surface to which nascent polypeptides are recruited. Since this surface also corresponds to the interface between the aggregate with its surroundings, it may be that proteins bound to the surface of the aggregate are in dynamic exchange. To address whether the recruiting surface of huntingtin corresponds to a site of transient or stable interaction with cellular proteins with distinctive dynamic properties compared with its dense core, we employed dynamic imaging methods of FRAP and FLIP (14, 38). The fluorescence of YFP alone recovered immediately as expected for a soluble cytoplasmic protein, and likewise the fluorescence of diffuse httQ78-YFP in cells without visible aggregates also recovered rapidly (Fig. 3, *A* and *D*, and data not shown). In contrast, no recovery was detected for httQ78-YFP in either the "ring" structure or the core (Fig. 3, *B* and *D*). We next examined the dynamic properties of TBP-YFP association with htt-78-CFP and observed that the TBP-YFP

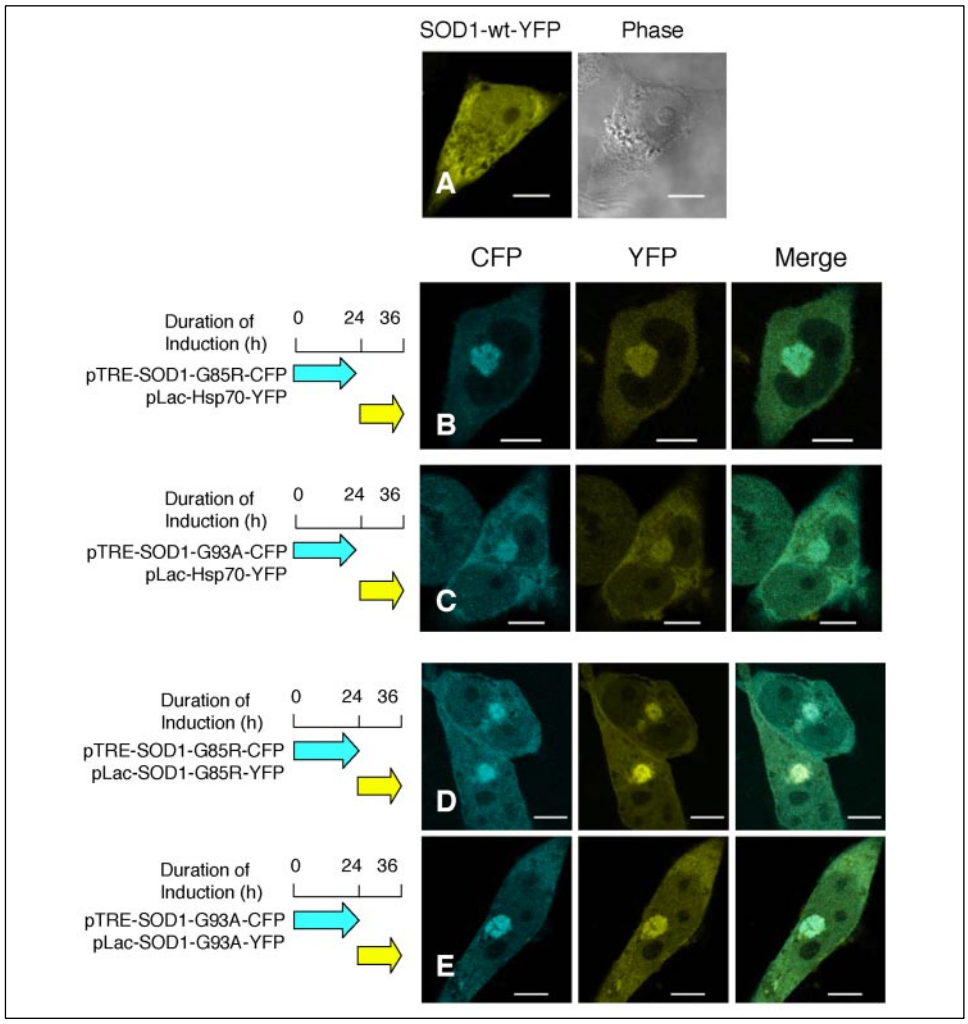

FIGURE 4. **SOD1-G85R and SOD1-G93A aggregates form a growth interface throughout the aggregate.** HeTOFLI was transfected with pTRE-SOD1-wt-YFP alone (*A*), pTRE-SOD1-G85R-CFP and pLac-Hsp70-YFP (*B*), pTRE-SOD1-G93A-CFP and pLac-Hsp70-YFP (*C*), pTRE-SOD1-G85R-CFP and pLac-SOD1-G85R-YFP (*D*), or pTRE-SOD1-G93A-CFP and pLac-SOD1-G93A-YFP (*E*). Sequential protein expression was induced as indicated. Cells with mutant SOD1 aggregates (*CFP*) and YFP-fused Hsp70, SOD1-G85R, or SOD1-G93A (*YFP*) were visualized by confocal microscopy. Co-localization was illustrated by merging CFP and YFP images (*Merge*). *Scale bar*, 10 μm.

fluorescent signal associated with the surface of httQ78-CFP aggregate also did not recover following photobleaching (Fig. 3, *C* and *D*). These results suggest an infrequent exchange between the proteins bound to the surface of huntingtin aggregates and the surrounding environment or between the surface and the core of the aggregate.

To demonstrate directly that the recruiting surface sequesters the associated proteins, we performed FLIP analysis of the httQ78-YFP ring. The fluorescence intensity of httQ78-YFP at the "ring" structure was monitored, since an area adjacent to the aggregate was photobleached. Using this method, dissociation of protein from the aggregate would result in decreased fluorescence intensity of the "ring" structure over time. Rather, we observed that the httQ78-YFP fluorescence signal persisted throughout the period of photobleaching, consistent with a conclusion that httQ78-YFP is stably bound. In contrast, the fluorescence of YFP alone diminished rapidly, consistent with our expectation that YFP is a soluble protein that does not interact with the aggregate (Fig. 3, *E–G*). Taken together, the FRAP and FLIP results reveal that proteins recruited to the exterior surface of huntingtin aggregates are stably and irreversibly associated.

Mutant SOD1 (G85R/G93A) Forms Porous Aggregate Structures—We next examined whether the organization and structural properties of the recruitment surface in polyglutamine-expansion huntingtin aggregates are typical of other aggregation-prone mutant proteins, such as mutant SOD1 aggregates (SOD1-G85R-Y/CFP and SOD1-G93A-Y/CFP) associated with familial amyotrophic lateral sclerosis (21, 22, 46). Whereas wild type SOD1 fused to YFP (SOD1-wt-YFP) is diffuse throughout the cell (similar to YFP alone; Fig. 4*A*), expression of either mutant SOD1-G85R-YFP or SOD1-G93A-YFP results in the appearance of large perinuclear cytoplasmic aggregates or inclusions (Fig. 4, *B–E*). To monitor interactions of mutant SOD1 aggregates with other cellular proteins, we focused on Hsp70, since neither TBP nor CBP co-localize with SOD1 aggregates (data not shown). Sequential expression of SOD1-G85R-CFP or SOD1-G93A-CFP followed by Hsp70-YFP showed co-localization of Hsp70 in a diffuse pattern throughout the entire region bounded by the SOD1 aggregate (Fig. 4, *B* and *C*). Likewise, sequential expression of SOD1-G85R-CFP and SOD1-G85R-YFP (or SOD1-G93A-CFP and SOD1-G93A-YFP) exhibited a similar diffuse pattern of co-localization, suggesting that mutant SOD1 also self-associates throughout the aggregate (Fig. 4, *D* and *E*). We have previously observed that aggregates formed by expression of mutant SOD1 are partially mobile (47). Taken together, these results suggest that mutant SOD1 forms porous structures *in vivo* with diffuse sites distributed throughout the aggregate to which other cellular proteins can associate.

Huntingtin and SOD1 Aggregates Form Distinct Intracellular Structures—We next examined whether a basis for differences in the structure of mutant huntingtin and SOD1 aggregates can be discerned using FRET analysis. We reasoned that detection of a FRET signal would indicate molecular interactions between associated molecules perhaps indicative of either ordered or organized structures. As expected, no FRET signal was detected in cells co-expressing soluble diffused

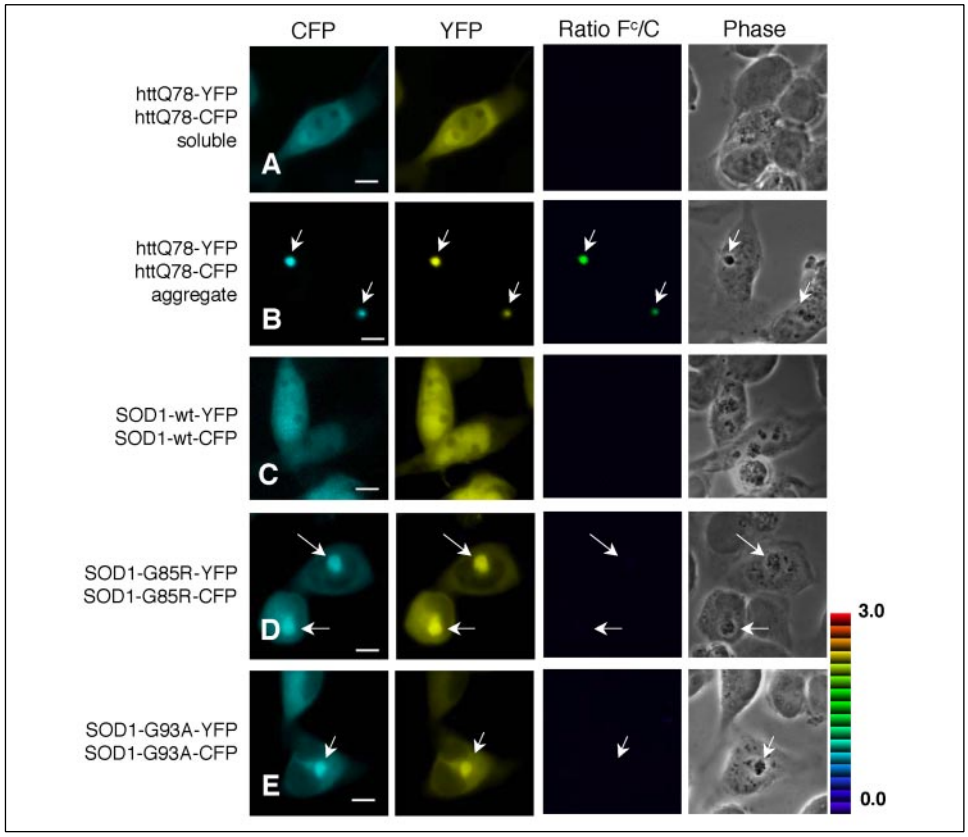

FIGURE 5. **FRET analysis of mutant huntingtin and SOD1 aggregate.** HeTOFLI were co-transfected with constructs encoding httQ78-CFP and httQ78-YFP (*A* and *B*), SOD1-wt-CFP and SOD1-wt-YFP (*C*), SOD1-G85R-CFP and SOD1-G85R-YFP (*D*), or SOD1-G93A-CFP and SOD1-G93A-YFP (*E*). Transfected cells with CFP (*CFP*) and YFP fusion proteins (*YFP*) were visualized by fluorescence microscopy. *Arrows*, mutant huntingtin or mutant SOD1 aggregates. The FRET ratio image represents the ratio between corrected FRET and CFP images, ranging from 0 to 3 (*Ratio F^c/C*). *Scale bar*, 10 μm.

httQ78-YFP and httQ78-CFP, httQ23-YFP and httQ23-CFP, or YFP and CFP (Fig. 5*A* and data not shown). However, aggregate structures in cells co-expressing httQ78-YFP and httQ78-CFP (Fig. 5*B*) or httQ23-YFP with httQ78-CFP showed intense FRET signals both in the core and at the surface (supplemental Fig. S3*A*). In contrast, no significant FRET signal was detected in aggregates containing huntingtin and associated cellular proteins, TBP, CBP, or Hsp70 (supplemental Fig. S3, *B–D*). These results reveal that the protein-protein interactions that define the huntingtin core differ substantially from the interactions at the surface of the aggregate with other cellular proteins.

Similar FRET experiments were performed with cells expressing wild-type SOD1 or mutant SOD1-G85R and SOD1-G93A aggregates. However, in no case did we detect any FRET signal either between mutant SOD1 molecules (Fig. 5, *C–E*). Therefore, in contrast to huntingtin, mutant SOD1 proteins do not form close molecular interactions in the aggregate, although the lack of a FRET signal in mutant SOD1 aggregates may also be due to the position of the fluorophores. Nevertheless, these results demonstrate that the intrinsic properties of mutant SOD1 are distinct from that observed for huntingtin aggregates.

DISCUSSION

Our *in vivo* studies on the molecular organization of an amino-terminal mutant huntingtin or mutant SOD1 expressed in human cells show striking differences in the organization and recruitment properties of the respective aggregate structures. We show that expression of huntingtin with expanded polyglutamine results in the appearance of structures with a dense core surrounded by interactive surfaces to which other glutamine-repeat containing cellular proteins are recruited stably. We describe three distinctive properties of the huntingtin core. 1) The preferential association between huntingtin molecules, consistent with an intense FRET signal, suggests that the core is a densely packed structure. 2) The core is inaccessible to other soluble cellular proteins. 3) The exterior of the core is a recruitment surface for interaction with other soluble proteins. The dense core could be formed by the collapse of soluble huntingtin into oligomers that self-associate to form structures to which other huntingtin monomers or oligomers are further recruited to form even larger aggregate structures (26, 48, 49). We show that the recruitment surface serves for both self-association with nascent huntingtin molecules and association with other cellular polyglutamine-containing proteins. However, because the interactions between huntingtin proteins and other cellular proteins at the recruitment surface do not exhibit any FRET signal, this suggests that sequestered proteins at the recruitment surface are not organized in the same manner as within the core. Further growth of the aggregate occurs by a combination of interactions of huntingtin self-association with the core and huntingtin association with other cellular proteins. Our living cell imaging studies of aggregates offer an understanding of electron micrographic observations of cells with huntingtin aggregates that have described a dense protein core and a less defined amorphous ring-like shell (50, 51). A number of cell biological studies using immunofluorescence have also indicated that huntingtin aggregates in fixed cells are inaccessible to antibodies and that only proteins at the surface are accessible (14, 18, 51–54). Our results showing that the core is inaccessible are also consistent with these observations and provide a basis to understand this phenomena.

In contrast to the ordered huntingtin aggregate structures described here, mutant SOD1 aggregates share none of these characteristics and instead form a diffuse porous structure. The dynamic features of mutant SOD1 allow for the rapid movement of both SOD1 and other cellular proteins through the porous aggregate (47). Unlike huntingtin, SOD1 does not exhibit any FRET signal *in vivo* (Fig. 5, *D* and *E*), interact with Congo red, or form highly organized fibrils *in vitro* (55–57). Based on a

direct comparison of mutant huntingtin and SOD1 proteins, the structures formed by these proteins are different in all biochemical and biophysical properties. We suggest that these distinct biochemical properties may affect the *in vivo* toxicity of mutant huntingtin or SOD1. Huntingtin aggregates contain a single exterior surface surrounding the core to which other cellular proteins can associate, whereas mutant SOD1 aggregates contain sites throughout the aggregate to which other cellular proteins can associate. For aggregates containing mutant SOD1, this could result in more aberrant interaction and sequestration of cellular proteins. Even among different proteins with polyglutamine expansions, divergent aggregate dynamics have been observed. Ataxin-1, for example, exhibits relatively fast mobility, whereas Ataxin-3 and huntingtin are immobile (52, 58). These observations suggest that the sequences flanking the polyglutamine motif could have a critical role in influencing aggregate structure.

The appearance of aggregates *in vivo* reflects the dynamics of misfolded proteins on protein homeostasis. Whether induced by environmental stress or mutations, as occurs with huntingtin and SOD1, the appearance of misfolded proteins is suppressed under steady-state conditions via active refolding and degradation (11, 36). At some point, however, when the cellular milieu is challenged either by an imbalance of a particular folded intermediate or by a dysregulation of components required for protein homeostasis, mutant huntingtin and SOD1 proteins escape the protein misfolding quality control checkpoints and accumulate as aggregating species. In cells that constitutively express the misfolded protein, these aggregate structures grow and persist. The aggregation process, however, is reversible, as demonstrated by the apparent disappearance of aggregates following down-regulation of huntingtin expression in mice and cell culture; these results suggest that aggregates can be dissociated, degraded, or otherwise disposed (59, 60). Our demonstration that huntingtin aggregates have an exterior surface to which nascent proteins are recruited to support growth suggests that the maintenance of aggregates reflects equilibrium of constant addition and removal at this surface. Under conditions that promote disaggregation, we propose that this recruiting surface probably corresponds to sites where molecular chaperones and perhaps other protein remodeling activities have an active role to dissociate or limit aggregate growth.

The identification of an exterior surface on huntingtin aggregates for recruitment of cellular proteins also suggests a mechanism by which aggregate structures can be cleared from the cell. If the rates of disaggregation and *de novo* recruitment are in equilibrium, we would expect that the phenotypes of aggregate structures would persist. However, changes in the activities or levels of molecular chaperones or degradative machineries, could shift this equilibrium and influence whether aggregates are dynamic or inert structures. Whereas our studies offer a more exact understanding of the *in vivo* events that occur when huntingtin or mutant SOD1 is expressed, similar studies on other aggregation-prone proteins will provide critical information on the diversity and perhaps complexity of these subcellular protein structures.

Acknowledgments—We thank Dr. M. Macdonald for huntingtin constructs, Dr. Q. Liu for SOD1 constructs, Dr. R. H. Goodman for the CBP construct, Dr. W. Russin and the bioimaging facility at Northwestern University for technical support of microscopes, the cell imaging facility at Northwestern Medical School, and S. Fox and K. E. Staniszewski for technical support.

REFERENCES

1. Taylor, J. P., Hardy, J., and Fischbeck, K. H. (2002) *Science* **296,** 1991–1995
2. Caughey, B., and Lansbury, P. T., Jr. (2003) *Annu. Rev. Neurosci.* **2003,** 267–298
3. Bossy-Wetzel, E., Schwarzenbacher, R., and Lipton, S. A. (2004) *Nat. Med.* **10,** (suppl.) 2–9
4. Zoghbi, H. Y., and Orr, H. T. (2000) *Annu. Rev. Neurosci.* **23,** 217–247
5. Suhr, S. T., Senut, M. C., Whitelegge, J. P., Faull, K. F., Cuizon, D. B., and Gage, F. H. (2001) *J. Cell Biol.* **153,** 283–294
6. Hughes, R. E., and Olson, J. M. (2001) *Nat. Med.* **7,** 419–423
7. Ross, C. A. (2002) *Neuron* **35,** 819–822
8. Nagai, Y., Onodera, O., Chun, J., Strittmatter, W. J., and Burke, J. R. (1999) *Exp. Neurol.* **155,** 195–203
9. Schmidt, T., Lindenberg, K. S., Krebs, A., Schols, L., Laccone, F., Herms, J., Rechsteiner, M., Riess, O., and Landwehrmeyer, G. B. (2002) *Ann. Neurol.* **51,** 302–310
10. Cummings, C. J., Mancini, M. A., Antalffy, B., DeFranco, D. B., Orr, H. T., and Zoghbi, H. Y. (1998) *Nat. Genet.* **19,** 148–154
11. Muchowski, P. J. (2002) *Neuron* **35,** 9–12
12. Holmberg, C. I., Staniszewski, K. E., Mensah, K. N., Matouschek, A., and Morimoto, R. I. (2004) *EMBO J.* **23,** 4307–4318
13. Ravikumar, B., Vacher, C., Berger, Z., Davies, J. E., Luo, S., Oroz, L. G., Scaravilli, F., Easton, D. F., Duden, R., O'Kane, C. J., and Rubinsztein, D. C. (2004) *Nat. Genet.* **36,** 585–595
14. Kim, S., Nollen, E. A., Kitagawa, K., Bindokas, V. P., and Morimoto, R. I. (2002) *Nat. Cell Biol.* **4,** 826–831
15. Huang, C. C., Faber, P. W., Persichetti, F., Mittal, V., Vonsattel, J. P., MacDonald, M. E., and Gusella, J. F. (1998) *Somat. Cell Mol. Genet.* **24,** 217–233
16. Schaffar, G., Breuer, P., Boteva, R., Behrends, C., Tzvetkov, N., Strippel, N., Sakahira, H., Siegers, K., Hayer-Hartl, M., and Hartl, F. U. (2004) *Mol. Cell* **15,** 95–105
17. Steffan, J. S., Kazantsev, A., Spasic-Boskovic, O., Greenwald, M., Zhu, Y.-Z., Gohler, H., Wanker, E. E., Bates, G. P., Housman, D. E., and Thompson, L. M. (2000) *Proc. Natl. Acad. Sci. U. S. A.* **97,** 6763–6768
18. Nucifora, F. C., Jr., Sasaki, M., Peters, M. F., Huang, H., Cooper, J. K., Yamada, M., Takahashi, H., Tsuji, S., Troncoso, J., Dawson, V. L., Dawson, T. M., and Ross, C. A. (2001) *Science* **291,** 2423–2428
19. Dunah, A. W., Jeong, H., Griffin, A., Kim, Y., Standaert, D. G., Hersch, S. M., Mouradian, M. M., Young, A. B., Tanese, N., and Krainc, D. (2002) *Science* **296,** 2238–2243
20. Li, S.-H., Cheng, A. L., Zhou, H., Lam, S., Rao, M., Li, H., and Li, X.-J. (2002) *Mol. Cell. Biol.* **22,** 1277
21. Bruijn, L. I., Houseweart, M. K., Kato, S., Anderson, K. L., Anderson, S. D., Ohama, E., Reaume, A. G., Scott, R. W., and Cleveland, D. W. (1998) *Science* **281,** 1851–1854
22. Cleveland, D. W., and Rothstein, J. D. (2001) *Nat. Rev.* **2,** 806–819
23. Reid, S. J., Roon-Mom, W. M. C. v., Wood, P. C., Rees, M. I., Owen, M. J., Faull, R. L. M., Dragunow, M., and Snell, R. G. (2004) *Brain Res. Mol. Brain Res.* **125,** 120–128
24. Ii, K., Ito, H., Tanaka, K., and Hirano, A. (1997) *J. Neuropathol. Exp. Neurol.* **56,** 125–131
25. Soto, C. (2003) *Nat. Rev. Neurosci.* **4,** 49–60
26. Scherzinger, E., Sittler, A., Schweiger, K., Heiser, V., Lurz, R., Hasenbank, R., Bates, G. P., Lehrach, H., and Wanker, E. E. (1999) *Proc. Natl. Acad. Sci. U. S. A.* **96,** 4604–4609
27. Chen, S., Berthelier, V., Hamilton, J. B., O'Nuallain, B., and Wetzel, R. (2002) *Biochemistry* **41,** 7391–7399
28. Chen, S., Berthelier, V., Yang, W., and Wetzel, R. (2001) *J. Mol. Biol.* **311,** 173–182
29. Poirier, M. A., Li, H., Macosko, J., Cai, S., Amzel, M., and Ross, C. A. (2002) *J. Biol. Chem.* **277,** 41032–41037
30. Stenoien, D. L., Cummings, C. J., Adams, H. P., Mancini, M. G., Patel, K., DeMartino, G. N., Marcelli, M., Weigel, N. L., and Mancini, M. A. (1999) *Hum. Mol. Genet.* **8,** 731–741
31. Becker, M., Martin, E., Schneikert, J., Krug, H. F., and Cato, A. C. (2000) *J. Cell Biol.* **149,** 255–262
32. Chen, H. K., Fernandez-Funez, P., Acevedo, S. F., Lam, Y. C., Kaytor, M. D., Fernandez, M. H., Aitken, A., Skoulakis, E. M., Orr, H. T., Botas, J., and Zoghbi, H. Y. (2003) *Cell* **113,** 457–468
33. Emamian, E. S., Kaytor, M. D., Duvick, L. A., Zu, T., Tousey, S. K., Zoghbi, H. Y., Clark, H. B., and Orr, H. T. (2003) *Neuron* **38,** 375–387
34. Urushitani, M., Kurisu, J., Tateno, M., Hatakeyama, S., Nakayama, K., Kato, S., and Takahashi, R. (2004) *J. Neurochem.* **90,** 231–244
35. Shimizu, N., Asakawa, S., Minoshima, S., Kitada, T., Hattori, N., Matsumine, H., Yokochi, M., Yamamura, Y., and Mizuno, Y. (2000) *J. Neural Transm. Suppl.* 19–30
36. Goldberg, A. L. (2003) *Nature* **426,** 895–899
37. Kwok, R. P., Laurance, M. E., Lundblad, J. R., Goldman, P. S., Shih, H., Connor, L. M., Marriott, S. J., and Goodman, R. H. (1996) *Nature* **380,** 642–646
38. Lippincott-Schwartz, J., Snapp, E., and Kenworthy, A. (2001) *Nat. Rev. Mol. Cell. Biol.* **2,** 444–456
39. Gordon, G. W., Berry, G., Liang, X. H., Levine, B., and Herman, B. (1998) *Biophys. J.* **74,** 2702–2713
40. Goldberg, Y. P., Nicholson, D. W., Rasper, D. M., Kalchman, M. A., Koide, H. B., Graham, R. K., Bromm, M., Kazemi-Esfarjani, P., Thornberry, N. A., Vaillancourt, J. P., and Hayden, M. R. (1996) *Nat. Genet.* **13,** 442–449
41. DiFiglia, M., Sapp, E., Chase, K. O., Davies, S. W., Bates, G. P., Vonsattel, J. P., and

Aronin, N. (1997) *Science* **277,** 1990–1993
42. Patterson, G. H., Schroeder, S. C., Bai, Y., Weil, A., and Piston, D. W. (1998) *Yeast* **14,** 813–825
43. Chen, D., Hinkley, C. S., Henry, R. W., and Huang, S. (2002) *Mol. Biol. Cell* **13,** 276–284
44. Chong, J. A., Moran, M. M., Teichmann, M., Kaczmarek, J. S., Roeder, R., and Clapham, D. E. (2005) *Mol. Cell. Biol.* **25,** 2632–2643
45. Boisvert, F. M., Kruhlak, M. J., Box, A. K., Hendzel, M. J., and Bazett-Jones, D. P. (2001) *J. Cell Biol.* **152,** 1099–1106
46. Rosen, D. R., Siddique, T., Patterson, D., Figlewicz, D. A., Sapp, P., Hentati, A., Donaldson, D., Goto, J., O'Regan, J. P., Deng, H. X., Rahmani, Z., Krizus, A., McKenna-Yasek, D., Cayabyab, A., Gaston, S. M., Berger, R., Tanzi, R. E., Halperin, J. J., Herzfeldt, B., Van den Bergh, R., Hung, W. Y., Bird, T., Deng, G., Mulder, D. W., Smyth, C., Laing, N. G., Soriano, E., Pericak-Vance, M. A., Haines, J., Rouleau, G. A., Gusella, J. S., Horvitz, H. R., and Brown, R. J., Jr. (1993) *Nature* **362,** 59–62
47. Matsumoto, G., Stojanovic, A., Holmberg, C. I., Kim, S., and Morimoto, R. I. (2005) *J. Cell Biol.* **171,** 75–85
48. Kazantsev, A., Walker, H. A., Slepko, N., Bear, J. E., Preisinger, E., Steffan, J. S., Zhu, Y., Gertler, F. B., Housman, D. E., Marsh, J. L., and Thompson, L. M. (2002) *Nat. Genet.* **30,** 367–376
49. Apostol, B. L., Kazantsev, A., Raffioni, S., Illes, K., Pallos, J., Bodai, L., Slepko, N., Bear, J. E., Gertler, F. B., Hersch, S., Housman, D. E., Marsh, L., and Thompson, L. M. (2003) *Proc. Natl. Acad. Sci. U. S. A.* **100,** 5950–5955
50. Hazeki, N., Tsukamoto, T., Yazawa, I., Koyama, M., Hattori, S., Someki, I., Iwatsubo, T., Nakamura, K., Goto, J., and Kanazawa, I. (2002) *Biochem. Biophys. Res. Commun.* **294,** 429–440
51. Qin, Z.-H., Wang, Y., Sapp, E., Cuiffo, B., Wanker, E., Hayden, M. R., Kegel, K. B., Aronin, N., and DiFiglia, M. (2004) *J. Neurosci.* **24,** 269–281
52. Chai, Y., Shao, J., Miller, V. M., Williams, A., and Paulson, H. L. (2002) *Proc. Natl. Acad. Sci. U. S. A.* **99,** 9310–9315
53. Waelter, S., Boeddrich, A., Lurz, R., Scherzinger, E., Lueder, G., Lehrach, H., and Wanker, E. E. (2001) *Mol. Biol. Cell* **12,** 1393–1407
54. Jiang, H., Nucifora, F. C. J., Ross, C. A., and DeFranco, D. B. (2003) *Hum. Mol. Genet.* **12,** 1–12
55. Scherzinger, E., Lurz, R., Turmaine, M., Mangiarini, L., Hollenbach, B., Hasenbank, R., Bates, G. P., Davies, S. W., Lehrach, H., and Wanker, E. E. (1997) *Cell* **90,** 549–558
56. Rakhit, R., Cunningham, P., Furtos-Matei, A., Dahan, S., Qi, X.-F., Crow, J. P., Cashman, N. R., Kondejewski, L. H., and Chakrabartty, A. (2002) *J. Biol. Chem.* **277,** 47551–47556
57. Okamoto, K., Hirai, S., Yamazaki, T., Sun, X. Y., and Nakazato, Y. (1991) *Neurosci. Lett.* **129,** 233–236
58. Stenoien, D. L., Mielke, M., and Mancini, M. A. (2002) *Nat. Cell. Biol.* **4,** 806–810
59. Yamamoto, A., Lucas, J. J., and Hen, R. (2000) *Cell* **101,** 57–66
60. Martin-Aparicio, E., Yamamoto, A., Hernandez, F., Hen, R., Avila, J., and Lucas, J. J. (2001) *J. Neurosci.* **21,** 8772–8781